Applied Mathematics Letters 107 (2020) 106426

Contents lists available at ScienceDirect

Applied Mathematics Letters

www.elsevier.com/locate/aml

Solving boundary value problems on manifolds with a plane waves method

Carlos J.S. Alves [a,*], Pedro R.S. Antunes [b], Nuno F.M. Martins [c], Svilen S. Valtchev [a,d]

[a] *CEMAT, Instituto Superior Técnico, ULisboa, 1049-001 Lisboa, Portugal*
[b] *Universidade Aberta & GFM-FCUL, University of Lisbon, Portugal*
[c] *Department of Mathematics, FCT - Universidade Nova de Lisboa, Caparica, Portugal*
[d] *Department of Mathematics, ESTG, Polytechnic of Leiria, Portugal*

ARTICLE INFO

Article history:
Received 9 March 2020
Received in revised form 20 April 2020
Accepted 20 April 2020
Available online 24 April 2020

Keywords:
Meshfree method
Plane waves method
Helmholtz–Beltrami operator
Manifolds

ABSTRACT

In this paper we consider a plane waves method as a numerical technique for solving boundary value problems for linear partial differential equations on manifolds. In particular, the method is applied to the Helmholtz–Beltrami equations. We prove density results that justify the completeness of the plane waves space and justify the approximation of domain and boundary data. A-posteriori error estimates and numerical experiments show that this simple technique may be used to accurately solve boundary value problems on manifolds.

1. Introduction

There has been a significant amount of recent results addressing the approximation of surface data (e.g. [1]), but as pointed out in [2], not much research work has been dedicated to the numerical solution of boundary value problems (BVP) for partial differential equations (PDE) on manifolds. Nevertheless, we mention some recent works with surface finite elements (cf. [3]) and with a method of particular solutions (cf. [4]) for eigenproblems for the Laplace–Beltrami operator. We have already considered the method of fundamental solutions on a sphere, cf. [5], and here we further extend the use of meshfree methods, by using a plane waves method, e.g. [6,7]. We prove density results for BVPs posed on a sphere or cylinder, and illustrate the accuracy of the proposed method through numerical experiments.

* Corresponding author.
E-mail addresses: carlos.alves@math.tecnico.ulisboa.pt (C.J.S. Alves), prantunes@ciencias.ulisboa.pt (P.R.S. Antunes), nfm@fct.unl.pt (N.F.M. Martins), ssv@math.ist.utl.pt (S.S. Valtchev).

https://doi.org/10.1016/j.aml.2020.106426
0893-9659/

1.1. General setting

Consider a connected and bounded domain $\Omega \subset \mathbb{R}^N$ with a C^2 boundary $\Gamma = \partial\Omega$, which defines a manifold of dimension $N-1$. Let $\omega \subset \Gamma$ be an open subset in the manifold with a C^1 boundary $\gamma = \partial\omega$, with respect to the topology of Γ. Our admissible domains assume that the complement of Ω is connected (thus, Ω may be a torus), and there is no particular restriction on ω (it may have several connected components or it may be multiply connected).

In this setting, we consider BVPs of the form

$$(\mathscr{P}) \begin{cases} \mathcal{D}_S(u) = f & \text{in } \omega \\ \mathcal{B}_S(u) = g & \text{on } \gamma, \end{cases} \tag{1}$$

where $\mathcal{D}_S$ is a linear differential operator on the manifold Γ and $\mathcal{B}_S$ is a linear boundary operator on γ. We assume that $(\mathscr{P})$ is well-posed in an appropriate functional setting, with an estimate

$$|||u|||_\omega \leq C_1\|f\|_\omega + C_2\|g\|_\gamma, \tag{2}$$

for some constants $C_1, C_2 > 0$, that do not depend on the data f, g, and where the norms are considered in that functional setting.

Considering an approximation of the form

$$\tilde{u}(x) = \sum_{k=1}^{K} \alpha_k \phi_k(x) \tag{3}$$

we obtain a discretized version of the problem

$$(\tilde{\mathscr{P}}) \begin{cases} \sum_{k=1}^K \alpha_k \mathcal{D}_S\phi_k(x) = f(x) & (x \in \omega), \\ \sum_{k=1}^K \alpha_k \mathcal{B}_S\phi_k(x) = g(x) & (x \in \gamma). \end{cases} \tag{4}$$

Using a collocation method with interior nodes $z_1, \ldots, z_M \in \omega$ and boundary nodes $x_1, \ldots, x_B \in \gamma$, we obtain the linear system

$$\mathbf{M}\boldsymbol{\alpha} = \mathbf{v} \Leftrightarrow \begin{bmatrix} \mathcal{D}_S\phi_1(z_1) & \cdots & \mathcal{D}_S\phi_K(z_1) \\ \vdots & \ddots & \vdots \\ \mathcal{D}_S\phi_1(z_M) & \cdots & \mathcal{D}_S\phi_K(z_M) \\ \mathcal{B}_S\phi_1(x_1) & \cdots & \mathcal{B}_S\phi_K(x_1) \\ \vdots & \ddots & \vdots \\ \mathcal{B}_S\phi_1(x_B) & \cdots & \mathcal{B}_S\phi_K(x_B) \end{bmatrix} \begin{bmatrix} \alpha_1 \\ \vdots \\ \alpha_K \end{bmatrix} = \begin{bmatrix} f(z_1) \\ \vdots \\ f(z_M) \\ g(x_1) \\ \vdots \\ g(x_B) \end{bmatrix}. \tag{5}$$

The matrix $\mathbf{M}$ has dimension $(M+B) \times K$, and if $M + B > K$ we may use the pseudo-inverse given with a Tikhonov regularization parameter $\tau > 0, \tau \approx 0$, to overcome ill-conditioning issues,

$$(\tau\mathbf{I} + \mathbf{M}^\star\mathbf{M})\boldsymbol{\alpha} = \mathbf{M}^\star\mathbf{v}. \tag{6}$$

Having obtained an approximation of the solution $\tilde{u}$ with the parameters α_k, the error satisfies

$$\begin{cases} \mathcal{D}_S(u-\tilde{u}) = f - \tilde{f} & \text{in } \omega, \\ \mathcal{B}_S(u-\tilde{u}) = g - \tilde{g} & \text{on } \gamma, \end{cases} \quad \text{with } \tilde{f} = \mathcal{D}_S(\tilde{u}),\ \tilde{g} = \mathcal{B}_S(\tilde{u}). \tag{7}$$

Therefore, we may obtain an *a posteriori* error estimate

$$|||u - \tilde{u}|||_\omega \leq C_1\|f - \tilde{f}\|_\omega + C_2\|g - \tilde{g}\|_\gamma. \tag{8}$$

1.2. Helmholtz–Beltrami BVP

As an example, in this paper we focus on the Helmholtz–Beltrami equation with a Dirichlet boundary condition

$$\begin{cases} \Delta_S u + \mu^2 u = f & \text{in } \omega \subset \partial\Omega \subset \mathbb{R}^3, \\ u = g & \text{on } \gamma = \partial\omega, \end{cases} \tag{9}$$

where $\mu \geq 0$ is a frequency (or wavenumber). We assume that $-\mu^2$ is not a Dirichlet eigenvalue of the Laplace–Beltrami operator in ω, which implies the well posedness of problem (9).

The surface gradient ∇_S is defined using a projection at each surface point $x \in \omega$,

$$P_x = I - \hat{n}(x)\hat{n}(x)^\top \implies \nabla_S v(x) = P_x \nabla v(x),$$

where $\hat{n}(x)$ is the outward unitary normal vector with respect to the domain boundary $\Gamma = \partial\Omega$. The Laplace–Beltrami operator is given by (e.g.[1])[1]

$$\Delta_S u = \Delta u - H_S \partial_{\hat{n}} u - \partial^{[2]}_{\hat{n}} u, \text{ with } H_S = P_x : \nabla\hat{n},\ \partial_{\hat{n}} u = \hat{n}^\top \nabla u,\ \partial^{[2]}_{\hat{n}} u = \hat{n}^\top (\nabla^2 u)\hat{n}.$$

2. Plane waves approximation

Consider plane waves basis functions of the form (here $\lambda > 0$ can be different from μ)

$$\phi(x) = \exp(\mathrm{i}\lambda \mathrm{w} \cdot x),$$

for some unitary directions $\mathrm{w} \in \partial B(0,1)$. Then,

$$\nabla_S \phi = P_x \nabla\phi = \mathrm{i}\lambda(\mathrm{w} - \hat{n}(\mathrm{w}.\hat{n}))\phi \tag{10}$$

$$\Delta_S \phi + \mu^2 \phi = \left(\mu^2 - \lambda^2 - \mathrm{i}\lambda(\mathrm{w}\cdot\hat{n})H_S + \lambda^2(\mathrm{w}\cdot\hat{n})^2\right)\phi = Q^{\mathrm{w}}_\Gamma \phi \tag{11}$$

with $H_S = (\mathbf{I} - \hat{n}\hat{n}^\top) : (\nabla\hat{n})$, and the function Q^{w}_Γ depends on the direction w and Γ.

The calculation of Q^{w}_Γ is given by formula (11) and only vectorial computations are needed, as long as expressions for $\hat{n}$ and $\nabla\hat{n}$ are available. Next, we present two examples where this calculation is explicit, but for C^2 parametric surfaces it would also be possible to calculate Q^{w}_Γ numerically.

Example 2.1. Case of a unit sphere $\Omega = B(0,1)$: we have $\hat{n}(x) = x$ and $H_S = N - 1$

$$\Delta_S \phi(x) + \mu^2\phi(x) = \left(\mu^2 - \lambda^2 + \mathrm{i}\lambda(1-N)(\mathrm{w}\cdot\hat{n}) + \lambda^2(\mathrm{w}\cdot\hat{n})^2\right)\phi(x).$$

Thus, in the 3D case, we get $Q^{\mathrm{w}}_\Gamma(x) = \mu^2 - \lambda^2 + (\lambda(\mathrm{w}\cdot x) - \mathrm{i})^2 + 1$.

Example 2.2. Consider the case of a cylinder in 3D,

$$\Omega = \{x \in \mathbb{R}^3 : |\tilde{x}| < 1, |x_3| < R + 1\}, \tag{12}$$

with $\tilde{x} = (x_1, x_2, 0) = \hat{n}(x)$ and $H_S = N - 2 = 1$. Take $\omega \subset \{x \in \partial\Omega : |x_3| < R\}$, then

$$\Delta_S \phi(x) = \left(\mu^2 - \lambda^2 - \mathrm{i}\lambda(\mathrm{w}\cdot\hat{n}) + \lambda^2(\mathrm{w}\cdot\hat{n})^2\right)\phi(x).$$

Thus, $Q^{\mathrm{w}}_\Gamma(x) = \mu^2 - \lambda^2 + \left(\lambda(\mathrm{w}\cdot\tilde{x}) - \frac{1}{2}\mathrm{i}\right)^2 + \frac{1}{4}$.

2.1. Plane waves system

Consider $\tilde{u}$ in (3) with $\phi_k(x) = \exp(\mathrm{i}\lambda \mathrm{w}_k \cdot x)$. At the domain collocation points, $z_j \in \omega$, we impose

$$(\Delta_S + \mu^2)\tilde{u}(z_j) = \sum_{k=1}^{K} \alpha_k Q^{\mathrm{w}_k}_\Gamma(z_j) \exp(\mathrm{i}\lambda \mathrm{w}_k \cdot z_j) = f(z_j) \quad (j = 1, \ldots, M), \tag{13}$$

[1] Here ∇^2 stands for the Hessian matrix and : for the real matrix dot product $A : B = \mathrm{tr}(A^\top B)$.

and at the boundary collocation points $x_j \in \partial\omega$,

$$\tilde{u}(x_j) = \sum_{k=1}^{K} \alpha_k \exp(\mathrm{i}\lambda \mathrm{w}_k \cdot x_j) = g(x_j), \quad (j = 1, \dots, B). \tag{14}$$

Combining (13) and (14) as a linear system (5) $\mathbf{M}\boldsymbol{\alpha} = \mathbf{v}$, we obtain the coefficient vector $\boldsymbol{\alpha}$ in the Tikhonov regularization sense (6). Thus, the approximation

$$\tilde{u}_K(x) = \sum_{k=1}^{K} \alpha_k \exp(\mathrm{i}\lambda w_k \cdot x) \tag{15}$$

minimizes the residual at the collocation points, in a regularized least-squares sense.

Remark 2.3. As mentioned in Section 1, the system could be built for other type of basis functions, and it might be possible to consider fundamental solutions (or RBFs) as basis functions. The advantage of considering plane waves is that the expressions of the derivatives are much simpler, and are explicitly given in some cases (see Examples 2.1 and 2.2).

Remark 2.4. Note that $\tilde{u}_K$ is a solution of the Helmholtz equation in the whole space

$$\Delta\tilde{u}_K + \lambda^2\tilde{u}_K = 0.$$

Therefore, here we are considering approximations to the Helmholtz–Beltrami BVP in ω that are solutions of a Helmholtz equation in Ω. When $\mu > 0$ we may use $\lambda = \mu$.

2.2. Density results

Theorem 2.5. *Consider $p \in \{0, 1, 2\}$, $\lambda > 0$, $q_p \neq 0$ a.e. in ω, an admissible $\omega \subset \partial\Omega \subset \mathbb{R}^3$, with*

$$\mathscr{S}_p = span\{(\mathrm{w} \cdot \hat{n})^p q_p \phi_{\mathrm{w}}|_\omega : \mathrm{w} \in \partial B(0,1)\} \tag{16}$$

and $\phi_{\mathrm{w}}(x) = e^{\mathrm{i}\lambda \mathrm{w}\cdot x}$. Then, each set $\mathscr{S}_p$ is dense in $L^2(\omega)$.

Proof. Take Φ the fundamental solution of the Helmholtz equation in $\mathbb{R}^3$ and the orientable crack ω, where the following single layer ($p = 0$) and double layer ($p = 1$) potentials (e.g. [8]) are defined,

$$u_p(x) = \int_\omega \alpha_p(y) q_p(y) \partial^p_{\hat{n}(y)} \Phi(x - y) ds_y. \tag{17}$$

With $\hat{x} = x/|x|$, note that when $r = |x| \to \infty$,

$$4\pi\partial_{\hat{n}(y)}\Phi(x-y) = \left(\frac{1}{|x-y|} - \mathrm{i}\lambda\right)\hat{n}\cdot\frac{x-y}{|x-y|}\frac{e^{\mathrm{i}\lambda|x-y|}}{|x-y|} \to -\mathrm{i}\lambda(\hat{n}\cdot\hat{x})\frac{e^{-\mathrm{i}\lambda\hat{x}\cdot y}}{r} + O(r^{-2}).$$

For $p = 2$ the hypersingular potential (17) is defined for Neumann problems in cracks, in the weak sense or using Cauchy principal values. We now use the forward difference approximation of the second derivative

$$\begin{aligned} 4\pi\partial^2_{\hat{n}(y)}\Phi(x-y) + O(\varepsilon) &= \frac{4\pi}{\varepsilon^2}\left(\Phi(x-y) - 2\Phi(x-y-n(y)\varepsilon) + \Phi(x-y-2n(y)\varepsilon)\right), \\ (|x| \to \infty) &\to \frac{1}{\varepsilon^2|x|}\left(\phi_{-\hat{x}}(y) - 2\phi_{-\hat{x}}(y+n(y)\varepsilon) + \phi_{-\hat{x}}(y+2n(y)\varepsilon)\right), \end{aligned}$$

and when $\varepsilon \to 0$ this gives $-\lambda^2(\hat{n}\cdot\hat{x})^2\phi_{-\hat{x}}(y)\frac{1}{r}$. Thus, u_p generates the far field

$$u_{p,\infty}(\hat{x}) = \frac{(-\mathrm{i}\lambda)^p}{4\pi}\int_\omega \alpha_p(y) q_p(y)(\hat{n}\cdot\hat{x})^p\phi_{-\hat{x}}(y) ds_y \quad \hat{x} \in \partial B(0,1).$$

To prove that $\mathscr{S}_p$ is dense in $L^2(\omega)$ we show that $\mathscr{S}_p^{\perp} = \{0\}$. This means that,

$$\text{if } \langle \alpha_p,\, q_p(\mathrm{w}\cdot\hat{n})^p \phi_{\mathrm{w}} \rangle_{L^2(\omega)} = 0,\ \forall \mathrm{w} \in \partial B(0,1), \quad \text{implies } \alpha_p = 0,$$

then the density is proven. The hypothesis means that the far field $u_{p,\infty}$ is null, and due to Rellich's lemma (e.g. [8]), this implies that u is null everywhere outside the crack ω. Therefore the jumps are null through the crack, i.e. $\alpha_p q_p = 0$, and since $q_p \neq 0$ this implies $\alpha_p = 0$, a.e. in ω. □

Remark 2.6. The density results presented here justify the possibility of directly approximating the solution, considering

$$Q_{\Gamma}^{\mathrm{w}}(x) = q_0(x) + q_1(x)(\mathrm{w}\cdot\hat{n}(x)) + q_2(x)(\mathrm{w}\cdot\hat{n}(x))^2.$$

This includes the sphere (Example 2.1) and the cylinder (Example 2.2).

Remark 2.7. These density results are presented here for cracks ω, meaning that $\omega \neq \Gamma$ and $\gamma \neq \emptyset$. However, it is worth observing that they also hold for $\omega = \Gamma$ if λ is not a resonance frequency for the Laplace operator in Ω.

3. Numerical simulations

We now consider some examples that illustrate the performance of the method. In the following we use the distribution of $K = 6L^2 + 2$ directions on the sphere (e.g.[6]),

$$\begin{aligned} w_{00}^{\pm} &= (0,0,\pm 1),\ \theta_k = \frac{k\pi}{2L},\ \tau_{jk} = \frac{j\pi}{3k}, \\ w_{jk}^{\pm} &= \left(\sin(\theta_k)\cos(\tau_{jk}), \sin(\theta_k)\sin(\tau_{jk}), \pm\cos(\theta_k)\right), \end{aligned} \tag{18}$$

with $j = 1,\ldots,6k$, and $k = 1,\ldots,L$ (and note that $\pm\cos(\theta_L) = 0$).

We will use the following notation:

$$\begin{aligned} \text{Error} &= \|u - \tilde{u}_K\|_{\infty,\bar{\omega}}, \\ \text{Residual} &= \max\{\|f - \mathcal{D}(\tilde{u}_K)\|_{\infty,\bar{\omega}}\ ,\ \|g - \tilde{u}_K\|_{\infty,\gamma}\}. \end{aligned}$$

Example 3.1. Let $\Omega = B(0,1)$ and $\omega = \{x \in \partial\Omega : x_3 > \ell\}$ (see Fig. 1), with $\ell = \cos(3\pi/8)$.

(a) First we consider problem (9) with a known solution, namely a spherical harmonic,

$$\mu = \sqrt{12} \approx 3.46,\ u(x) = 4\sqrt{2\pi/35}\, Y_{3,3}(x) = x_1^3 - x_1 x_2^2,\ f = 0,\ g = u.$$

Using $M = 817$ collocation points in ω and $B = 256$ points on $\gamma = \partial\omega$, we obtained

K	Residual ($\lambda = 3$)	Error ($\lambda = 3$)	Residual ($\lambda = 4$)	Error ($\lambda = 4$)
98	1.7×10^{-6}	3.3×10^{-8}	3.5×10^{-5}	6.7×10^{-7}
152	2.1×10^{-7}	3.6×10^{-8}	3.4×10^{-8}	1.0×10^{-8}
296	3.3×10^{-7}	1.0×10^{-7}	4.9×10^{-8}	1.2×10^{-8}

(b) We now consider problem (9) with an unknown solution, taking

$$\mu = 1,\ f(x) = 8(x_3 - 4x_1^2 + x_2),\ g = 0.$$

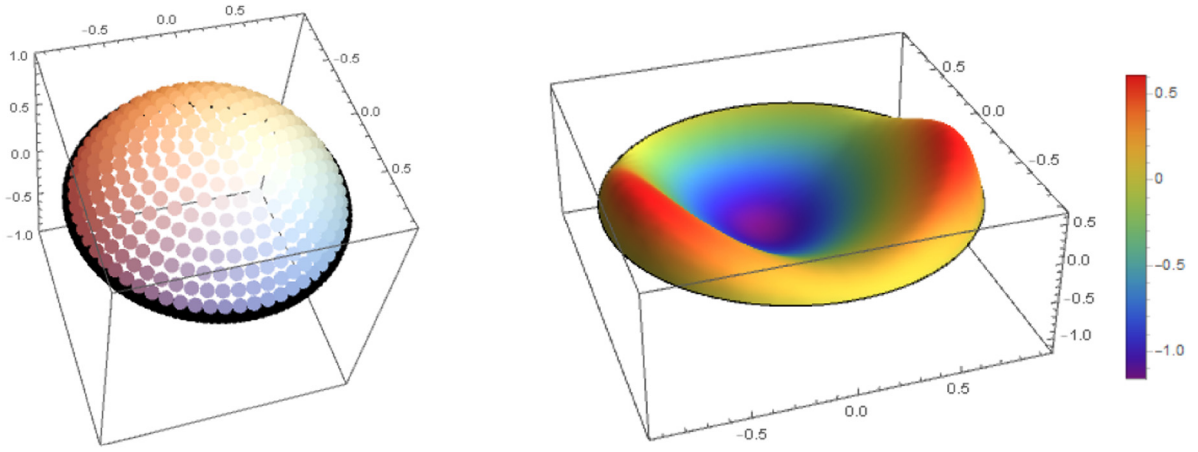

Fig. 1. Example 3.1: On the left, the geometry with collocation points (black points are on the boundary). On the right, the approximate solution $\tilde{u}_{296}$ using $\lambda = 4$.

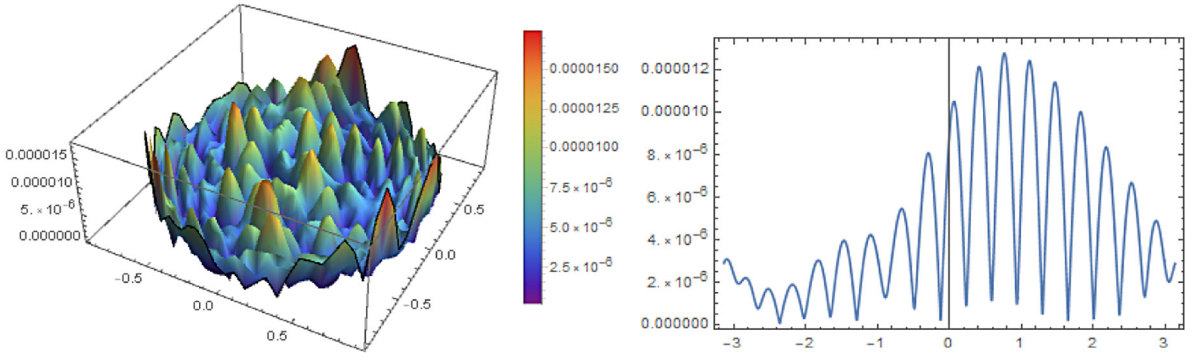

Fig. 2. Example 3.1: Residual error in the domain (on the left). Error on the boundary (on the right), as a function of the angle..

The solution is plotted in Fig. 1, on the right, using the coordinates $(x_1, x_2, \tilde{u}_K(x))$ with $x \in \bar{\omega}$. A table with results for $M = 2977$, $B = 256$ is presented here:

K	Residual ($\lambda = 2$)	Residual ($\lambda = 3$)	Residual ($\lambda = 4$)
152	1.8×10^{-4}	0.6×10^{-4}	1.2×10^{-4}
296	3.0×10^{-4}	2.2×10^{-4}	0.2×10^{-4}
488	4.8×10^{-4}	0.4×10^{-4}	0.8×10^{-4}

In Fig. 2 (on the left) we plot the residual error in the domain, and in Fig. 2 (on the right) we plot the error on the boundary.

As it can be seen from the results presented in the tables, there is no trivial relation between the increase of the number K, of plane waves, and the accuracy of the method, which we believe is related to the numerical precision problems in solving the ill-conditioned systems.

Example 3.2. We now consider a cylinder Ω as defined in (12), using $R = 1$. The collocation points on the cylinder ω are presented in Fig. 3 (left). We consider the BVP (9) with

$$\mu = \lambda = 3,\ f = 0,\ \text{and}\ g(x) = \begin{cases} x_1 & if\ x_3 = 1, \\ x_2 & if\ x_3 = -1. \end{cases}$$

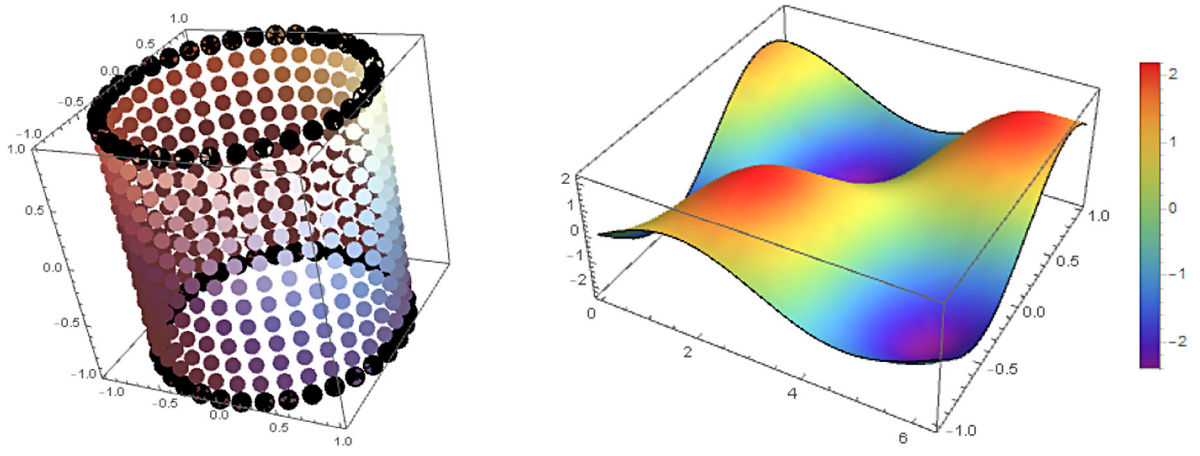

Fig. 3. Example 3.2: On the left, a geometry with the collocation points (black points are on the boundary). On the right, the approximate solution u_{296}.

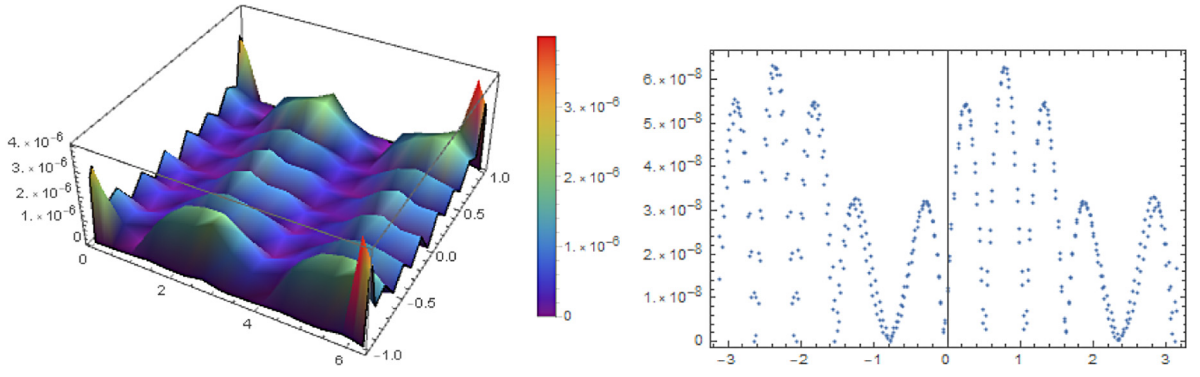

Fig. 4. Example 3.2: Residual in the domain (on the left), and error on the boundaries (on the right)..

In order to illustrate the accuracy of the method, also in this geometry, we considered $M = 468$, $B = 144$, and the approximate solution u_K with $K = 296$ is plotted in Fig. 3, on the right. The residual in the domain is less than 5×10^{-6} and the error on the boundary is less than 6.5×10^{-8} (see Fig. 4).

4. Conclusions

In this paper we demonstrate that the plane waves method may be used as a simple and accurate method to solve boundary value problems for partial differential equations on manifolds. Illustrative numerical examples for Helmholtz–Beltrami Dirichlet BVPs show the accuracy of the method.

We focused on the Dirichlet problem for the Helmholtz–Beltrami equation, but the method can be extended for the Neumann or Robin problems, and to several other linear PDEs. The implementation can be performed for other surfaces. The sphere and the cylinder might also be used to explore axisymmetric features of the method (cf. [7]).

Acknowledgments

The financial support of the Portuguese Fundação para a Ciência e a Tecnologia (FCT), through the projects UIDB/04621/2020 and UIDP/04621/2020 of CEMAT/IST-ID (first, third and fourth author) and PTDC/MAT-CAL/4334/2014 (second author), is gratefully acknowledged.

References

[1] K.C. Cheung, L. Ling, A kernel-based embedding method and convergence analysis for surfaces PDEs, SIAM J. Sci. Comput. 40 (1) (2018) A266–A287.
[2] C. Piret, The orthogonal gradients method: A radial basis functions method for solving partial differential equations on arbitrary surfaces, J. Comput. Phys. 231 (14) (2012) 4662–4675.
[3] A. Bonito, A. Demlow, J. Owen, A priori error estimates for finite element approximations to eigenvalues and eigenfunctions of the Laplace–Beltrami operator, SIAM J. Numer. Anal. 56 (5) (2018) 2963–2988.
[4] J. Dahne, B. Salvi, Computation of tight enclosures for Laplacian eigenvalues, 2020, arXiv.org/abs/2003.08095.
[5] C.J.S. Alves, P.R.S. Antunes, The method of fundamental solutions applied to boundary value problems on the surface of a sphere, Comput. Math. Appl. 75 (7) (2018) 2365–2373.
[6] C.J.S. Alves, S.S. Valtchev, Numerical comparison of two meshfree methods for acoustic wave scattering, Eng. Anal. Bound. Elem. 29 (4) (2005) 371–382.
[7] A. Karageorghis, The plane waves method for axisymmetric Helmholtz problems, Eng. Anal. Bound. Elem. 66 (2016) 46–56.
[8] D. Colton, R. Kress, Inverse Acoustic and Electromagnetic Scattering Theory, Springer-Verlag GmbH, 2012.